THE JOURNAL OF PHYSICAL CHEMISTRY B

Article

pubs.acs.org/JPCB

Side-Chain Dynamics Reveals Transient Association of Aβ_{1-40} Monomers with Amyloid Fibers

Janarthanan Krishnamoorthy, Jeffrey R. Brender, Subramanian Vivekanandan, Nicole Jahr, and Ayyalusamy Ramamoorthy*

Biophysics and Department of Chemistry, University of Michigan, Ann Arbor, Michigan 48109-1055, United States

Supporting Information

ABSTRACT: Low-lying excited states that correspond to rare conformations or transiently bound species have been hypothesized to play an important role for amyloid nucleation. Despite their hypothesized importance in amyloid formation, transiently occupied states have proved difficult to detect directly. To experimentally characterize these invisible states, we performed a series of Carr−Purcell−Meiboom−Gill (CPMG)-based relaxation dispersion NMR experiments for the amyloidogenic Aβ_{1-40} peptide implicated in Alzheimer's disease. Significant relaxation dispersion of the resonances corresponding to the side-chain amides of Q15 and N27 was detected before the onset of aggregation. The resonances corresponding to the peptide backbone did not show detectable relaxation dispersion, suggesting an exchange rate that is not within the practical limit of detection. This finding is consistent with the proposed "dock and lock" mechanism based on molecular dynamics simulations in which the Aβ_{1-40} monomer transiently binds to the Aβ_{1-40} oligomer by non-native contacts with the side chains before being incorporated into the fiber through native contacts with the peptide backbone.

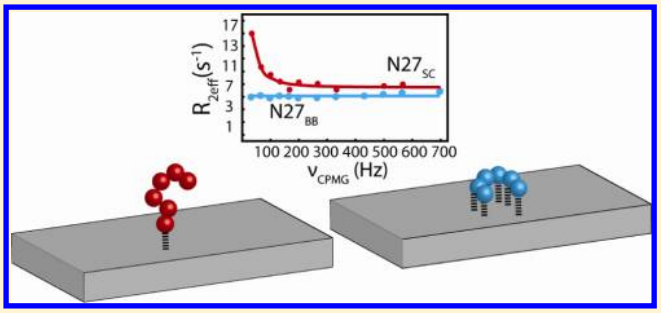

INTRODUCTION

Amyloid fibers are typically formed in a multistep process that is highly dependent on the formation of energetically unfavorable nuclei.[1] It has been noted that many amyloid proteins are neither completely unfolded nor structured like globular proteins but rather share many characteristics of premolten globule proteins.[2−6] Proteins in the premolten globule state possess transient secondary structure, are more compact than random coil proteins, and possess some hydrophobic clusters as revealed by ANS binding.[2,7] Consistent with this, NMR studies have predicted a range of possible structures for monomeric Aβ depending on the initial conditions ranging from almost completely disordered,[8,9] a conformation possessing long-range contacts but devoid of secondary structure described as a collapsed coil,[10] a largely unfolded conformation possessing a central turn,[11,12] and a hairpin-like structure possessing a well-defined 3_{10} helix.[13] This multiplicity of possible structures is in agreement with simulations that predict Aβ, like many other intrinsically disordered proteins, exists as an ensemble of rapidly interconverting, nearly isoenergetic, conformational species.[14] The monomeric Aβ peptide is therefore believed to exist in a variety of conformational states, some of which are aggregation prone and act as nuclei for amyloid formation.[11,12,15−17] In addition to the conformational polymorphism of the Aβ monomer, Aβ also oligomerizes at low concentrations even before the onset of fiber formation to form dimers, trimers, and high-molecular-weight nonfibrillar oligomers.[18−20] Because of their central role in controlling amyloid formation, the transitions occurring between putative amyloid precursors have been a subject of considerable interest and speculation.[21] Direct structural information has been noticeably absent, as the transient nature and low abundance of the nucleating states has made it difficult to study by many biophysical methods.

Exchange between such low-lying excited states can be quantified using NMR spectroscopy.[22−24] An excited state undergoing conformational exchange with the native state dephases the transverse magnetization in an NMR experiment, which is manifested as broader, less intense lines in the spectrum and increased R_{2eff} relaxation rates.[25] This information can be used to probe the excited state by Carr−Purcell−Meiboom−Gill (CPMG) relaxation dispersion experiments that employ a train of 180° pulses to periodically refocus the chemical shift evolution, allowing the stochastic chemical exchange occurring between the ground and excited states to dephase the refocusing in a quantitative manner. Higher CPMG frequencies are more effective at refocusing the chemical shift to a degree that is dependent on the rate of exchange between states.[25] From a plot of the effective relaxation rate (R_{2eff}) versus the frequency of the CPMG refocusing pulses, the chemical shift difference between the excited and native state, the populations of each state, and the

Received: May 30, 2012
Revised: September 15, 2012
Published: November 1, 2012

   dx.doi.org/10.1021/jp305279w | J. Phys. Chem. B 2012, 116, 13618−13623

rate of exchange can theoretically be determined.[25−27] The CPMG experiment is remarkably sensitive to the presence of exchanging states; chemical shifts corresponding to an excited population as small as 0.5% of the total population can be measured provided the exchange happens on the millisecond to microsecond time scale.[28] In this study, our CPMG-based measurements show significant relaxation dispersion for the side-chain amide resonances but not for the corresponding backbone resonances. This difference in relaxation dispersion profiles indicates the amide groups of the side chains of Q15 and N27 participate in an exchange process that the backbone resonances do not, which we link to transient binding of the side chains monomeric $A\beta_{1-40}$ to the surface of a larger oligomer.

MATERIALS AND METHODS

NMR samples were prepared from ^{15}N-labeled $A\beta_{1-40}$ (rPeptide) by first dissolving the peptide in 1% ammonium hydroxide, lyophilizing, and then resuspending in 1 mM NaOH (pH 10). The peptide was then diluted with 10× NaPi−NaCl buffer for a final buffer concentration of 20 mM sodium phosphate, pH 7.3, with 50 mM NaCl, and a final peptide concentration of 230 μM. All data were acquired on a 900 MHz Bruker NMR spectrometer equipped with a cryogenic triple-resonance pulse-field gradient probe.

Proton diffusion NMR measurements were carried out using the stimulated echo (STE) bipolar pulsed field gradient (PFG) pulse sequence with squared gradient pulses of constant duration (2.5 ms) and a variable gradient amplitude along the longitudinal axis.[29] Other experimental parameters include a 90° pulse width of 13.4 μs, an eddy-current delay of 2 ms, a stimulated-echo delay of 200 ms, a recycle delay of 1 s, a spectral width of 11.68 kHz, and 8192 data points. A saturation pulse centered at the water ^{1}H resonance frequency was used for solvent suppression. Radio frequency pulses were phase cycled to remove unwanted echoes. All spectra were processed with 8 Hz exponential line broadening prior to Fourier transformation. The diffusion coefficients were determined from the slope of a log plot of the intensity as a function of gradient strength using the Stejskal−Tanner equation.[30] The hydrodynamic radius was then calculated from the diffusion coefficient using the Einstein−Stokes relation and the viscosity of water at 20 °C. The stability of the sample was confirmed by repeat measurements at the same gradient strength at different time points.

For the CPMG relaxation dispersion experiments, a constant-time, relaxation-compensated pulse sequence with a ^{1}H continuous wave spin-lock field applied during the ^{15}N CPMG π-pulse train was used, using a ^{15}N CPMG π-pulse width of 45 μs.[31] ^{15}N CPMG π-pulses were applied at the following frequencies (ν_{CPMG}), 0, 33.33, 66.66, 99.99, 133.33, 166.66, 200, 266.66, 333.33, 433.33, 500, 566.66, and 700 Hz, where $\nu_{CPMG} = 1/(4\tau)$ and τ = spin−echo delay. Data were zero-filled to 4096 points in both t_1 and t_2 and then Fourier transformed after applying a sine-bell-squared window function shifted between $\pi/2$ and $\pi/4$. A polynomial baseline correction was applied to both sides of the residual water signal. Each 2D spectrum was obtained using 128 t_1 experiments, 16 scans, and a 1.5 s recycle delay. 2D data were processed using TOPSPIN 2.1 (from Bruker) and NMRPipe.[32] Resonance assignments were performed using SPARKY 3.113, using published assignments for $A\beta_{1-40}$ as a guide.[13,33]

The relaxation dispersion curves were initially fit to the full Carver−Richards equation by nonlinear optimization using the Levenberg−Marquadt algorithm and an in-house C program.[34] Monte Carlo simulations of the χ^2 surface from a fit to the full Carver−Richards model showed a relatively strong dependence on k_{ex} and a strong interdependence of the other variables, leading to a reliable qualitative estimate for k_{ex} and unreliable predictions for other variables.

RESULTS

To quantify and characterize possible low-lying excited states in $A\beta_{1-40}$, we performed a series of CPMG-based relaxation dispersion experiments on 250 μM samples of $A\beta_{1-40}$ (20 mM KPi and 50 mM NaCl at pH 7.3) at three different temperatures (4, 15, and 20 °C). A constant time, relaxation-compensated pulse sequence was used for each experiment to minimize the effects of dipole−dipole cross-correlation effects and the interchanging of in-phase and antiphase magnetization due to scalar coupling.[31] 2D ^{1}H/^{15}N-HSQC experiments were performed before and after each CPMG experiment; the resemblance of these spectra indicates that changes in the relaxation dispersion profile can be directly interpreted as arising from conformational exchange and not as an artifact of peptide aggregation during the CPMG experiment (Figure S1 in the Supporting Information).

Efforts were made to perform the experiments in a buffer that is reasonably close to physiological conditions (near-neutral pH, moderate ionic strength). Under these conditions, previous studies have shown that $A\beta_{1-40}$ exists as a mixture of monomers and large nonfibrillar oligomers even at low concentrations.[18,35] This result was confirmed in our sample by STE-PFG experiments, which showed the majority of the resonances in the ^{1}H spectrum correspond to a quickly diffusing species with a hydrodynamic radius of 0.50 ± 0.01 nm (Figure 1B). This value is consistent with a small monomeric protein in a folded conformation, similar to a recent NMR structure of $A\beta_{1-40}$ under similar conditions (pdb 2LFM).[13] Traces of a larger oligomer can be detected as a broad peak near −0.5 ppm arising from strongly shielded methyl groups in the oligomer that is commonly found in the spectra of amyloidogenic proteins (Figure 1A).[35−38] In the STE-PFG spectra, this peak is associated with a hydrodynamic radius of 7.73 ± 0.08 nm (Figure 1C), consistent with measurements of several types of large oligomers commonly found in $A\beta_{1-40}$ samples such as amylospheroids.[39,40]

While the large oligomers are not directly observed in the CPMG relaxation experiments, the formation of a substantial population of NMR invisible oligomers results in a signal that is significantly lower than might be expected for the concentration used. Nevertheless, it was possible to accurately measure a relaxation dispersion profile for 33 out of 40 backbone amide resonances and the amide side-chain resonances of Q15 and N27.

As can be seen in Figures 2 and 3, the relaxation dispersion curves for the backbone resonances of $A\beta_{1-40}$ showed only a slight dependence on the CPMG frequency for all the temperatures studied (4, 15, and 20 °C). While the R_{2eff} values from the backbone amide protons were nearly independent of the CPMG frequency (Figure 3), a strong dependence was detected for the side-chain resonances detectable by HSQC (Figure 2). The R_{2eff} for the Q15 and N27 side-chain resonances decreased strongly as the CPMG frequency increased, consistent with conformational exchange for these

dx.doi.org/10.1021/jp305279w | J. Phys. Chem. B 2012, 116, 13618−13623

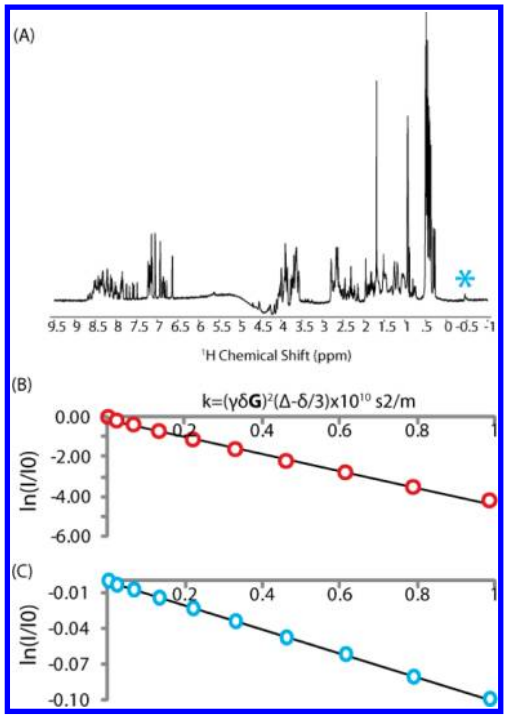

Figure 1. (A) Proton NMR spectrum of 230 μM Aβ_{1-40} at 20 °C in 20 mM sodium phosphate, pH 7.3, with 50 mM NaCl. The oligomer peak at −0.5 ppm is marked with an asterisk. The decay of the normalized stimulated-echo intensity obtained from STE-PFG ^{1}H NMR spectra calculated from the integrated volume of the peaks between 0.85 and 0.45 ppm (B) and −1.0 to −0.3 ppm (C) (marked with an asterisk in (A)).

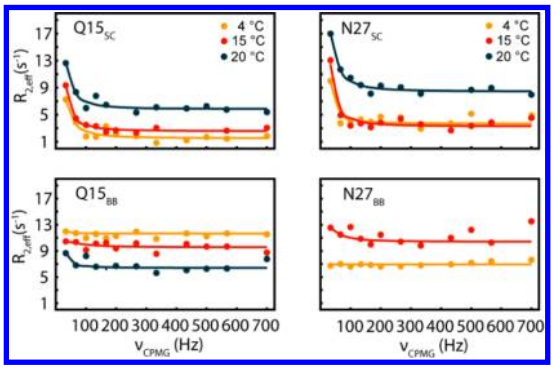

Figure 2. CPMG relaxation dispersion profiles for the amide side chain (top) and backbone (bottom) ^{15}N resonances of the Q15 and N27 residues of Aβ_{1-40} at 4, 15, and 20 °C. The relaxation dispersion profiles for the remainder of the backbone resonances can be found in Figure 3.

resonances in the microsecond to millisecond regime. The relaxation dispersion experiments therefore indicate that the side-chain amides of Q15 and N27 are undergoing exchange with another state, while a similar exchange process cannot be detected for the backbone amides of Aβ_{1-40}. The absence of a measurable relaxation dispersion for the backbone resonances of Aβ_{1-40} can arise from several factors: (a) the population of the excited state may be too small to be measured by CPMG ($\ll$0.5%); (b) the chemical environment of the backbone resonances in the excited state may be very similar to the ground state ($\Delta\omega \sim 0$); or (c) the exchange rate for the backbone resonances may be either too fast or too slow to be accurately quantified by CPMG.

In principle, the relaxation dispersion curve for the side-chain resonances can be fitted to a general two-state exchange model (the Carver−Richards equation)[34] to quantify the population of the excited state and the chemical shift difference rates of exchange between states. In practice, however, several factors complicate this analysis for Aβ_{1-40}.[41] First, the CPMG profile of the side-chain amide resonances only showed large relaxation dispersion within 100 Hz of the applied CPMG field strength, beyond which there is no significant variation in the $R_{2,\mathrm{eff}}$ value. Considering this limitation, the estimated parameters depend heavily on the initial three points, making a multiparameter fit to the data problematic. In principle, this difficulty can be partially overcome by additional measurements at a lower magnetic field.[41] However, in our case, the unusually low signal originating from the Aβ_{1-40} peptide made quantitative analysis at lower field strength difficult. Second, the R_2 value of the invisible excited state is not known a priori. While the Carver−Richards model is largely insensitive to this parameter for values moderately close to R_2 of the ground state,[42] the exchange process may involve oligomeric species of Aβ_{1-40}, which will consequently have an R_2 value differing greatly from the ground monomeric state.[43] Considering these limitations inherent to the Aβ_{1-40} system, we therefore did not attempt to rigorously quantitate the exchange kinetics between ground and excited states for the side-chain resonances from the CPMG experiment. While the chemical shift difference between states ($\Delta\omega$) and population of the excited state (p) could not be estimated even qualitatively from the data, it was possible, however, to qualitatively estimate k_{ex} for the side-chain resonances as being between 100 and 200 s^{-1} from fitting to an approximation to the Carver−Richards model considering a fast exchange regime.

While the relaxation dispersion experiments indicate the side-chain amides of Aβ_{1-40} are in exchange with a low-lying excited state, they do not provide a mechanism for the exchange process. Yamaguchi et al. have shown that a coil-to-turn conformational equilibrium within the Aβ_{1-40} monomer leads to an extreme broadening of the backbone resonances at higher temperatures.[11] To determine if a similar exchange process is responsible for the relaxation dispersion detected for the side-chain amides, we examined the effect of temperature on both the line shape and relaxation dispersion profiles of the backbone and side-chain resonances. At the lowest temperature (4 °C), minor peaks were found near many of the backbone resonances (see Figure S2 in the Supporting Information). Both the minor and major peaks broadened and disappeared as the temperature was increased (Figure S2), qualitatively reproducing the broadening effect of the backbone resonances reported by Yamaguchi et al.[11] By contrast, the variation of the relaxation dispersion profiles with temperature was primarily confined to a shift in the baseline at higher CPMG frequencies where $R_{2,\mathrm{eff}}$ is almost entirely independent of the applied CPMG frequency (Figures 2 and 3). A broad baseline reflects an increase in the transverse relaxation rate in the absence of chemical exchange (R_0) rather than a change in the exchange process, since the chemical shift difference between states is almost completely refocused at high CPMG frequencies. The absence of a significant temperature effect on the relaxation dispersion profile suggests an additional process is responsible for the chemical exchange detected for the side-chain amides by the relaxation dispersion experiment, and the temperature-dependent coil-to-turn conformational transition within the Aβ_{1-40} monomer is a separate process occurring on a much slower time scale.

dx.doi.org/10.1021/jp305279w | J. Phys. Chem. B 2012, 116, 13618−13623

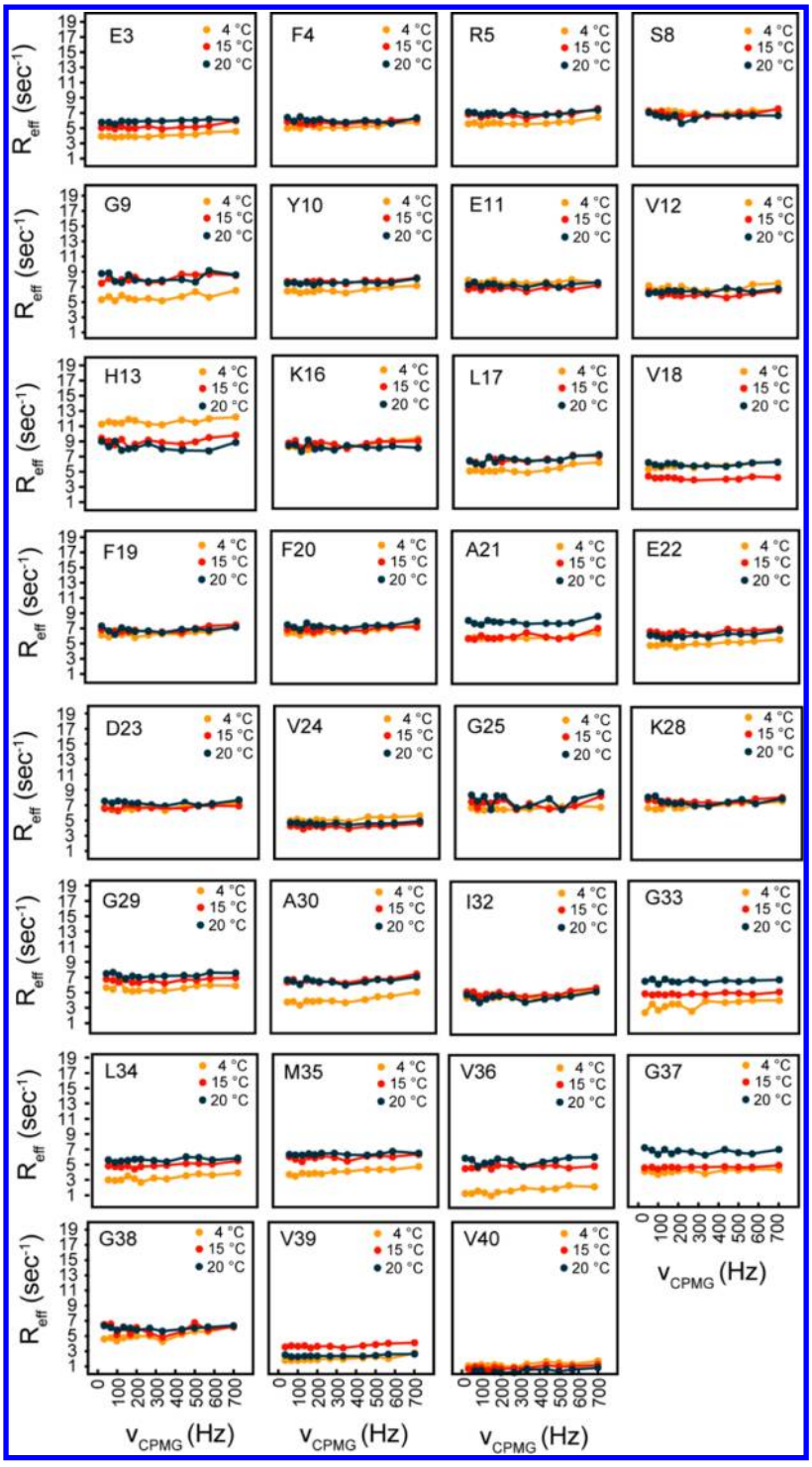

Figure 3. CPMG relaxation dispersion profiles of the backbone ^{15}N resonances of Aβ_{1-40} at 4, 15, and 20 °C. The relaxation dispersion profiles for the Q15 and N27 backbone resonances can be found in Figure 2.

DISCUSSION

While normally considered an irreversible process, the aggregation of Aβ_{1-40} and other amyloidogenic proteins actually proceeds by a large number of reversible steps.[44] Our results indicate the side-chain amides of Q15 and N27 participate in a dynamic process on the millisecond time scale, which is not found for the backbone resonances on that time scale. It is difficult to tell directly if the exchange results from an intramolecular conformational change within the monomeric peptide or from the intermolecular association of the Aβ_{1-40} monomer with an oligomeric species of Aβ_{1-40}. However, it is difficult to conceive of an intramolecular conformational change that only consists of alterations of side-chain chain conformations without concurrent changes in the conformation of the peptide backbone on the same time scale. Since the side chains of N27 and Q15 are spatially separated in all available models of the Aβ_{1-40} monomer,[8−13] a conformational change that brings them into contact must necessarily

dx.doi.org/10.1021/jp305279w | J. Phys. Chem. B 2012, 116, 13618−13623

involve an alteration of the backbone dihedral angles. Such a change would almost certainly be reflected in the relaxation dispersion profile of the backbone resonances due to the sensitivity of the ^{15}N chemical shift to the dihedral angle.

From these considerations, it is apparent that the millisecond exchange observed for the side-chain amide groups of N27 and Q15 is actually more likely the result of the association of the NMR detectable monomer with the larger NMR-invisible oligomer (Figure 1). At relatively low concentrations, the $A\beta_{1-40}$ monomer coexists with a large micelle-like, nonfibrillar aggregate (Figure 1C).[35−38] Similar micelle-like aggregates have been detected to coexist with the monomeric protein for other amyloidogenic proteins.[45−47] Saturation transfer based experiments have shown that the peptide backbone of a small fraction of the monomer population of $A\beta_{1-40}$ is in contact with these aggregates with an apparent k_{ex} rate of 76 s^{-1}.[43,48] The reversible association detected in these experiments is reflective of the first step of a two-stage "dock and lock" process in which the peptide transiently associates with aggregate, largely through contacts not native to the fiber, before forming strong native interactions.[49,50]

The relaxation profile observed for the N27 and Q15 side chains is consistent with this mechanism. Binding of the $A\beta_{1-40}$ monomer to the oligomer by contacts with the peptide backbone is characterized by a slow exchange rate and a small population of the bound state.[43,48] This finding is consistent with the flat relaxation dispersion profile detected for the peptide backbone, as the $R_{2,eff}$ value determined by CPMG relaxation dispersion is strongly dependent on both the exchange rate and population of the bound state. Therefore, the exchange rate for the backbone resonances is likely to be too slow to be detected by CPMG.[51] By contrast, the large relaxation dispersion observed for the N27 and Q15 side-chain amide resonance suggests relatively fast binding of these groups to the oligomer. It is important to note that the CPMG experiment relies on HSQC detection. For this reason, interactions with side chains not containing an amide group are not visible in the HSQC experiment and hence are not detectable in the CPMG experiment.

Molecular dynamics simulations have shown that the monomeric protein of $A\beta_{1-40}$ makes many transient non-native contacts ("docking") before thermodynamically stable native contacts can be formed ("locking").[50] An enhanced rate of docking is likely to translate into an enhanced rate of locking, as the peptide is more likely to make additional contacts once bound to the surface due to the close spatial proximity of the monomer to the surface of the oligomer and the conformational restriction within the monomer by binding to the oligomer. Stretches of amino acids containing asparagine and glutamine residues have a marked tendency to form amyloid, the most prominent example being the direct correspondence between polyglutamine repeats and amyloid formation in Huntington's disease.[52] The preponderance of asparagines and glutamine residue in amyloidogenic proteins has been commonly attributed to the increased thermodynamic stability of the fiber from intermolecular hydrogen bonding from the side chains of these residues.[53,54] However, our results raise the possibility that the high rate of transient association of asparagine and glutamine side chains in the monomer with the oligomer may also be a factor in amyloid formation. A comprehensive study comparing the association rates of asparagine and glutamine side chains with that of other side chains (which are invisible in the CPMG experiment) and to examine the effect of cofactors such as inhibitors and metal ions on association rates would be interesting in this context.[55−58]

■ ASSOCIATED CONTENT

Supporting Information

2D ^{1}H, ^{1}N HSQC spectra taken before and after the CPMG experiment and representative peaks from the HSQC experiments showing the temperature broadening effect. This material is available free of charge via the Internet at http://pubs.acs.org.

■ AUTHOR INFORMATION

Corresponding Author

*E-mail: ramamoor@umich.edu. Tel.: 734- 647-6572.

Notes

The authors declare no competing financial interest.

■ ACKNOWLEDGMENTS

This study was supported by research funds from NIH to A.R.

■ REFERENCES

(1) DeToma, A. S.; Salamekh, S.; Ramamoorthy, A.; Lim, M. H. *Chem. Soc. Rev.* **2012**, *41*, 608−621.
(2) Uversky, V. N.; Fink, A. L. *Biochim. Biophys. Acta* **2004**, *1698*, 131−153.
(3) Williamson, J. A.; Miranker, A. D. *Protein Sci.* **2007**, *16*, 110−117.
(4) Yonemoto, I. T.; Kroon, G. J.; Dyson, H. J.; Balch, W. E.; Kelly, J. W. *Biochemistry* **2008**, *47*, 9900−9910.
(5) Brender, J. R.; Salamekh, S.; Ramamoorthy, A. *Acc. Chem. Res.* **2012**, *45*, 454−462.
(6) Nanga, R. P. R.; Brender, J. R.; Vivekanandan, S.; Popovych, N.; Ramamoorthy, A. *J. Am. Chem. Soc.* **2009**, *131*, 17972−17979.
(7) Kayed, R.; Bernhagen, J.; Greenfield, N.; Sweimeh, K.; Brunner, H.; Voelter, W.; Kapurniotu, A. *J. Mol. Biol.* **1999**, *287*, 781−796.
(8) Riek, R.; Guntert, P.; Dobeli, H.; Wipf, B.; Wuthrich, K. *Eur. J. Biochem.* **2001**, *268*, 5930−5936.
(9) Hou, L. M.; Shao, H. Y.; Zhang, Y. B.; Li, H.; Menon, N. K.; Neuhaus, E. B.; Brewer, J. M.; Byeon, I. J. L.; Ray, D. G.; Vitek, M. P.; Iwashita, T.; Makula, R. A.; Przybyla, A. B.; Zagorski, M. G. *J. Am. Chem. Soc.* **2004**, *126*, 1992−2005.
(10) Zhang, S.; Iwata, K.; Lachenmann, M. J.; Peng, J. W.; Li, S.; Stimson, E. R.; Lu, Y.; Felix, A. M.; Maggio, J. E.; Lee, J. P. *J. Struct. Biol.* **2000**, *130*, 130−141.
(11) Yamaguchi, T.; Matsuzaki, K.; Hoshino, M. *FEBS Lett.* **2011**, *585*, 1097−1102.
(12) Lazo, N. D.; Grant, M. A.; Condron, M. C.; Rigby, A. C.; Teplow, D. B. *Protein Sci.* **2005**, *14*, 1581−1596.
(13) Vivekanandan, S.; Brender, J. R.; Lee, S. Y.; Ramamoorthy, A. *Biochem. Biophys. Res. Commun.* **2011**, *411*, 312−316.
(14) Sgourakis, N. G.; Merced-Serrano, M.; Boutsidis, C.; Drineas, P.; Du, Z. M.; Wang, C. Y.; Garcia, A. E. *J. Mol. Biol.* **2011**, *405*, 570−583.
(15) Yan, Y. L.; Liu, J. J.; McCallum, S. A.; Yang, D. W.; Wang, C. Y. *Biochem. Biophys. Res. Commun.* **2007**, *362*, 410−414.
(16) Lim, K. H.; Collver, H. H.; Le, Y. T. H.; Nagchowdhuri, P.; Kenney, J. M. *Biochem. Biophys. Res. Commun.* **2007**, *353*, 443−449.
(17) Lim, K. H.; Henderson, G. L.; Jha, A.; Louhivuori, M. *ChemBioChem* **2007**, *8*, 1251−1254.
(18) Narayanan, S.; Reif, B. *Biochemistry* **2005**, *44*, 1444−1452.
(19) Ding, H.; Wong, P. T.; Lee, E. L.; Gafni, A.; Steel, D. G. *Biophys. J.* **2009**, *97*, 912−921.
(20) Bitan, G.; Lomakin, A.; Teplow, D. B. *J. Biol. Chem.* **2001**, *276*, 35176−35184.
(21) Straub, J. E.; Thirumalai, D. *Annu. Rev. Phys. Chem.* **2011**, *62*, 437−463.

(22) Mukherjee, S.; Pondaven, S. P.; Jaroniec, C. P. *Biochemistry* **2011**, *50*, 5845−5857.
(23) Williamson, J. A.; Loria, J. P.; Miranker, A. D. *J. Mol. Biol.* **2009**, *393*, 383−396.
(24) Wei, L.; Jiang, P.; Yau, Y. H.; Summer, H.; Shochat, S. G.; Mu, Y. G.; Pervushin, K. *Biochemistry* **2009**, *48*, 2368−2376.
(25) Baldwin, A. J.; Kay, L. E. *Nat. Chem. Biol.* **2009**, *5*, 808−814.
(26) Mittermaier, A.; Kay, L. E. *Science* **2006**, *312*, 224−228.
(27) Mulder, F. A. A.; Mittermaier, A.; Hon, B.; Dahlquist, F. W.; Kay, L. E. *Nat. Struct. Biol.* **2001**, *8*, 932−935.
(28) Hansen, D. F.; Vallurupalli, P.; Lundstrom, P.; Neudecker, P.; Kay, L. E. *J. Am. Chem. Soc.* **2008**, *130*, 2667−2675.
(29) Tanner, J. E. *J. Chem. Phys.* **1970**, *52*, 2523−2526.
(30) Stejskal, E. O.; Tanner, J. E. *J. Chem. Phys.* **1965**, *42*, 288−292.
(31) Hansen, D. F.; Vallurupalli, P.; Kay, L. E. *J. Phys. Chem. B* **2008**, *112*, 5898−5904.
(32) Delaglio, F.; Grzesiek, S.; Vuister, G. W.; Zhu, G.; Pfeifer, J.; Bax, A. *J. Biomol. NMR* **1995**, *6*, 277−293.
(33) Yoo, S. I.; Yang, M.; Brender, J. R.; Subramanian, V.; Sun, K.; Joo, N. E.; Jeong, S. H.; Ramamoorthy, A.; Kotov, N. A. *Angew. Chem., Int. Ed.* **2011**, *50*, 5110−5115.
(34) Carver, J. P.; Richards, R. E. *J. Magn. Reson.* **1972**, *6*, 89−105.
(35) Sabate, R.; Estelrich, J. *J. Phys. Chem. B* **2005**, *109*, 11027−11032.
(36) Lomakin, A.; Chung, D. S.; Benedek, G. B.; Kirschner, D. A.; Teplow, D. B. *Proc. Natl. Acad. Sci. U.S.A.* **1996**, *93*, 1125−1129.
(37) Yong, W.; Lomakin, A.; Kirkitadze, M. D.; Teplow, D. B.; Chen, S. H.; Benedek, G. B. *Proc. Natl. Acad. Sci. U.S.A.* **2002**, *99*, 150−154.
(38) Lee, J.; Culyba, E. K.; Powers, E. T.; Kelly, J. W. *Nat. Chem. Biol.* **2011**, *7*, 602−609.
(39) Matsumura, S.; Shinoda, K.; Yamada, M.; Yokojima, S.; Inoue, M.; Ohnishi, T.; Shimada, T.; Kikuchi, K.; Masui, D.; Hashimoto, S.; et al. *J. Biol. Chem.* **2011**, *286*, 11555−11562.
(40) Noguchi, A.; Matsumura, S.; Dezawa, M.; Tada, M.; Yanazawa, M.; Ito, A.; Akioka, M.; Kikuchi, S.; Sato, M.; Ideno, S.; et al. *J. Biol. Chem.* **2009**, *284*, 32895−32905.
(41) Kovrigin, E. L.; Kempf, J. G.; Grey, M. J.; Loria, J. P. *J. Magn. Reson.* **2006**, *180*, 93−104.
(42) Ishima, R.; Torchia, D. A. *J. Biomol. NMR* **2006**, *34*, 209−219.
(43) Fawzi, N. L.; Ying, J.; Torchia, D. A.; Clore, G. M. *J. Am. Chem. Soc.* **2010**, *132*, 9948−9951.
(44) Kodaka, M. *Biophys. Chem.* **2004**, *107*, 243−253.
(45) Rhoades, E.; Gafni, A. *Biophys. J.* **2003**, *84*, 3480−3487.
(46) Soong, R.; Brender, J. R.; Macdonald, P. M.; Ramamoorthy, A. *J. Am. Chem. Soc.* **2009**, *131*, 7079−7085.
(47) Huang, R.; Vivekanandan, S.; Brender, J. R.; Abe, Y.; Naito, A.; Ramamoorthy, A. *J. Mol. Biol.* **2012**, *416*, 108−120.
(48) Fawzi, N. L.; Ying, J. F.; Ghirlando, R.; Torchia, D. A.; Clore, G. M. *Nature* **2011**, *480*, 268−272.
(49) Straub, J. E.; Thirumalai, D. *Curr. Opin. Struct. Biol.* **2010**, *20*, 187−195.
(50) Nguyen, P. H.; Li, M. S.; Stock, G.; Straub, J. E.; Thirumalai, D. *Proc. Natl. Acad. Sci. U.S.A.* **2007**, *104*, 111−116.
(51) Tollinger, M.; Skrynnikov, N. R.; Mulder, F. A. A.; Forman-Kay, J. D.; Kay, L. E. *J. Am. Chem. Soc.* **2001**, *123*, 11341−11352.
(52) Scherzinger, E.; Sittler, A.; Schweiger, K.; Heiser, V.; Lurz, R.; Hasenbank, R.; Bates, G. P.; Lehrach, H.; Wanker, E. E. *Proc. Natl. Acad. Sci. U.S.A.* **1999**, *96*, 4604−4609.
(53) DePace, A. H.; Santoso, A.; Hillner, P.; Weissman, J. S. *Cell* **1998**, *93*, 1241−1252.
(54) Fooks, H. M.; Martin, A. C. R.; Woolfson, D. N.; Sessions, R. B.; Hutchinson, E. G. *J. Mol. Biol.* **2006**, *356*, 32−44.
(55) Braymer, J. J.; Choi, J. S.; DeToma, A. S.; Wang, C.; Nam, K.; Kampf, J. W.; Ramamoorthy, A.; Lim, M. H. *Inorg. Chem.* **2011**, *50*, 10724−10734.
(56) Choi, J. S.; Braymer, J. J.; Nanga, R. P. R.; Ramamoorthy, A.; Lim, M. H. *Proc. Natl. Acad. Sci. U.S.A.* **2010**, *107*, 21990−21995.
(57) Hindo, S. S.; Mancino, A. M.; Braymer, J. J.; Liu, Y. H.; Vivekanandan, S.; Ramamoorthy, A.; Lim, M. H. *J. Am. Chem. Soc.* **2009**, *131*, 16663−16665.
(58) Jones, M. R.; Service, E. L.; Thompson, J. R.; Wang, M. C.; Kimsey, I. J.; Detoma, A. S.; Ramamoorthy, A.; Lim, M. H.; Storr, T. *Metallomics* **2012**, *4*, 910−920.